GESEP – Gerência de Especialistas em Sistemas Elétricos de Potência

Título:

Comparison of Current Grid Controllers in a DG Inverter with Grid Harmonic Distortion

Autores:

W. C. S. Amorim, D. C. Mendonça, J. M. S. Callegari, M. P. Silva, H. A. Pereira e A. F. Cupertino.

Publicado em:

13th IEEE/IAS International Conference on Industry Application (Induscon)

Data da Publicação:

2018

Citação para a versão publicada:

W. C. S. Amorim, D. C. Mendonça, J. M. S. Callegari, M. P. Silva, H. A. Pereira and A. F. Cupertino, " “Comparison of Current Grid Controllers in a DG Inverter with Grid Harmonic Distortion,” 13th IEEE/IAS International Conference on Industry Application (Induscon), São Paulo, 2018, pp. 1-8.

Comparison of Current Grid Controllers in a DG Inverter with Grid Harmonic Distortion

William Caires Silva Amorim
Department of Electrical Engineering
CEFET - MG
Belo Horizonte, Brazil
william.caires@ufv.br

Dayane do Carmo Mendonça
Department of Electrical Engineering
Federal University of Viçosa
Viçosa, Brazil
dayane.mendonca@ufv.br

João Marcus Soares Callegari
Department of Electrical Engineering
Federal University of Viçosa
Viçosa, Brazil
joao.callegari@ufv.br

Matheus Pereira Silva
Department of Electrical Engineering
Federal University of Viçosa
Viçosa, Brazil
matheus.p.silva10@gmail.com

Heverton Augusto Pereira
Department of Electrical Engineering
Federal University of Viçosa
Viçosa, Brazil
heverton.pereira@ufv.br

Allan Fagner Cupertino
Department of Materials Engineering
CEFET - MG
Belo Horizonte, Brazil
afcupertino@ieee.org

***Abstract*—This paper aims to present the analyzes of different grid current controllers applied in a full-bridge inverter used in distributed generation (DG). The presence of harmonic interaction in the grid, can be explained by the impedance-grid resonance problem between the equivalent grid impedance and the inverter impedance. The analyzes of different control strategies involve aspects such as power losses, quality of the current injected into the grid and dynamic performance during grid disturbances. In order to study the converter performance connected to the grid, it is made a comparison in this work by means of three controllers: proportional and integral (PI), proportional resonant (PR) and repetitive (RT). The simulation results show the higher efficiency of the PR and RT controllers in grid distorted conditions. The modulation techniques and discretization methods also affect the grid power quality, focusing in particular on the Bipolar technique. Therefore, this work proposes with these mechanisms to improve the performance of the operation DG grids, and consequently to increase the system power quality.**

***Index Terms*—Grid Harmonic Distortion, PI Controller, Repetitive Controller, Proportional Resonant Controller, Modulation Strategies, Discretization Methods.**

I. Introduction

In recent decades, new technologies for electric power generation have reached the market. Thus, it is expected an complexity integration into electricity systems, affecting the entire generation, transmission and distribution process [1]. Most of these technologies have an emphasis on generating energy from renewable sources, such as solar and wind energy [2]. With a strong appeal to reduce the environmental impact of power generation, the renewable sources carry the challenges of reducing the cost associated with the transmission system among diverse markets. Thus, the installation of power generation equipments near the places of consumption [3], and it is known as distributed generation (DG). DG technologies are applied in different systems and at different stages of development, such as photovoltaic systems, wind energy conversion systems, gas turbines, gas and diesel engines, fuel cell systems, among others [3], [4]. The advantages of this type of generation can be listed as [4]:

1) Reduction of transmission losses;
2) Increased global energy efficiency;
3) Relief of congestion in transmission and distribution lines;
4) Voltage support;
5) Deferred investments to upgrade, transmission and distribution systems.

Distributed power generation is one of the strongest characteristics of renewable energy sources, which connected to the grid, offers a series of advantages and flexibility to the generation and distribution system [5]. In many of these forms of energy, the inverter is responsible for the power electronic converters interface the grid and the power sources. However, high order harmonics are generated due to the inverter switching, requiring LC filters to attenuate these harmonics originated from the switching process. In addition, the other types of disturbances from the grid, make it difficult to control the connection of the inverter to the grid [6]. On the other hand, it is intended to synthesize higher quality energy, requiring more complex control strategies in order to maintain the stability of the system, especially in cases of resonant peaks [7].

The inverters are applied in photovoltaic systems and their presence in the point of connection (PoC) among the grid, significantly impacts the power quality [8], [9]. Besides, the presence of nonlinear loads is the other way to introduce distortion in the grid [10]. Although allowed to operate in an isolated circuit, when it is connected to the grid, there are distorted currents from the source and can change the characteristics in the PoC. [11]. The use of these loads is a major concern of both energy suppliers and consumers, and is a problem for the electrical system as a whole [12].

In this way, the conventional proportional and integral (PI) controller is one of the classic and traditional ways to suppress part of the harmonic current. On the other hand the proportional resonant (PR) and the repetitive (RT) controller, has the capability of reducing the non-fundamental current

The authors would like to thank the Brazilian agencies CNPq, CAPES and FAPEMIG by funding.

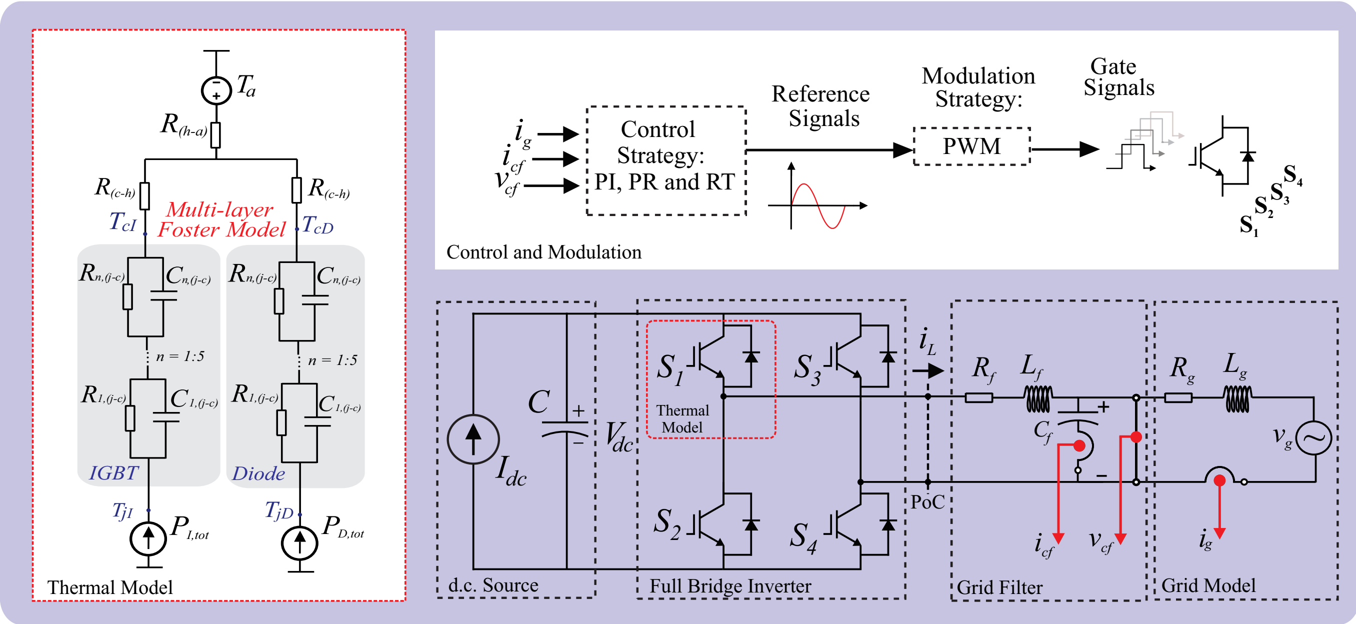

Fig. 1. Single-phase DG Inverter System

harmonic optimally [13]. The dual loop-loop control with feedforward is a simple control strategy, the system response is fast. Modulation strategies have also been well-regarded as to their results and impacts on grid quality as well as on inverter switches loss factors [14]. Challenges arise to maintain stability and eliminate high-order current harmonics in the grid when this is connected to inverters.

In this sense, this work is developed with the purpose of studying the impacts of modulation techniques and discretization methods on different types of grid current control. In this way, the study proposals of this work can be summarized:

1) Implement three types of grid current control for an inverter connected to the grid connected inverter;
2) Analyze the impact of modulation strategies and discretization methods in the controllers;
3) Benchmarking of the implemented controls, in terms of power losses, total demand distortion (TDD), total harmonic distortion (THD) and error in the grid current;
4) Control performance analysis in different short-circuit ratios;

This work is outlined as follows. Section II presents the single-phase DG inverter system. The control strategies and discretization methods are presented in Section III. Section IV presents the modulation strategies. Section V discusses the case study. In Section VI, the results are clearly stated and properly analyzed. Section VII presents the conclusion and final discussions.

II. Single-Phase DG Full Bridge Inverter System

In order to analyze the impact of the grid voltage harmonic distortion on the inverter, the grid model is implemented by means of an RL impedance, simplifying the characteristics of the transmission line. The inverter is coupled to the grid trough a LC filter (L_f and C_f) at the PoC. Fig. 1 shows the model of the single phase inverter connected to the system.

The inverter model is full bridge type and all switches are made up of IGBTs and diodes. The type of inverter chosen can be justified, by the ability to set higher voltage levels, with the same d.c.-link, in comparison with to the half bridge.

III. Strategy Control - Definitions

The control strategy studied in this work are presented in Fig. 2. The implemented loop control is designed for the grid current (i_g) and the capacitor current is measured for the active damping strategy (i_{C_f}) [21]; it is also used a feedforward in the v_{cf}, aiming to maintain the stability of the control, for all studied control strategies. The transfer functions $G_1(s)$ and $G_2(s)$ are shown in (1) and (2), respectively.

$$G_1(s) = \frac{sC_f}{L_fC_fs^2 + R_fC_fs + 1}. \tag{1}$$

$$G_2(s) = \frac{1}{s(L_gC_fs + R_gC_f)}. \tag{2}$$

In Fig. 3 (a) the PI controller is presented. The controller is discretized by three methods: Forward, Backward and Trapezoidal. The $G_{PI}(s)$ is defined as (in continuous mode):

$$G_{PI}(s) = K_{P1} + K_{I1}\frac{1}{s}, \tag{3}$$

where K_{P1} and K_{I1} are defined as [20]:

$$K_{P1} = (L_g + L_f)\frac{f_{sw}}{3}, \tag{4}$$

$$K_{I1} = 10(R_g + R_f)\frac{f_{sw}}{3}. \tag{5}$$

and f_{sw} is the switching frequency.

In Fig. 3 (b) the PR controller is shown. The controller is discretized by the Tustin with prewarping method. The controller G_{PR}(s) performs the attenuation at each characteristic frequency of *n-th* order, given by [15], [16] (in continuous mode):

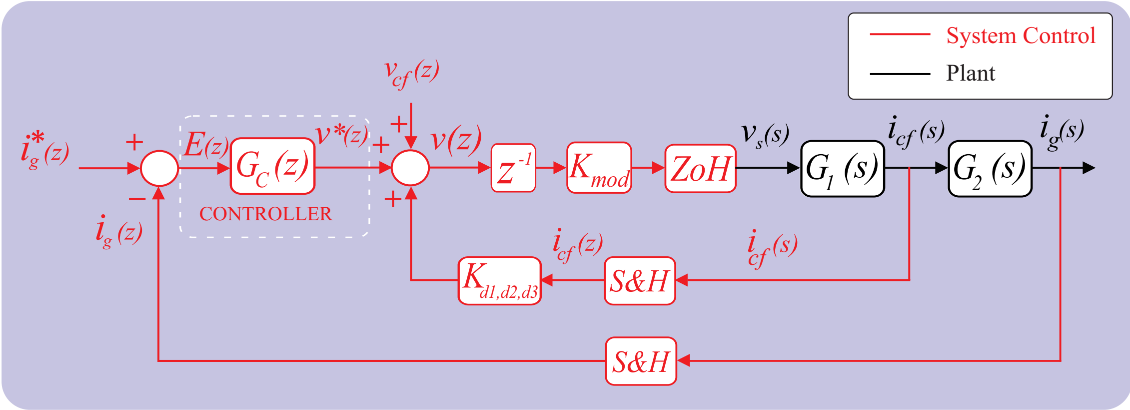

Fig. 2. Control Strategy.

$$G_{PR}(s) = K_{PR} + \sum_{n=1,\dots,N} K_{In} \frac{s}{s^2 + h_n^2 \omega_1^2}, \tag{6}$$

where K_{PR} is the proportional gain, defined in equation (7) [19], and K_{In} the integral resonant gain.

$$K_{PR} = \frac{1}{\sqrt{2}(1-\rho_o^{-1})}(R_f{+}R_g)\sqrt{2+2\rho_o^{-2}-\rho_o^{-1}(1+\sqrt{5})}, \tag{7}$$

where ρ_o is defined as:

$$\rho_o = e^{\frac{R_f+R_g}{(L_f+L_g)f_{sw}}}. \tag{8}$$

In this work, the PR controller was designed by n = 1, 5, 7, 11, 17 and 19.

In Fig. 3 (c) the RT controller is presented. The discretized controller $Q(z)$, $G_f(z)$ and proportional gain K_1 are defined in equations (9), (11) and (12), respectively.

$$Q(z) = \alpha_1 z + \alpha_0 + \alpha_1 z^{-1}, \tag{9}$$

where α_1 is expressed as:

$$\alpha_1 = \frac{1-\alpha_0}{2}, \tag{10}$$

$$G_f(z) = z^m, \tag{11}$$

$$K_1 = \frac{(Lg + L_f)f_{sw}}{3}, \tag{12}$$

The block diagram of RT controller can be reduced in terms of one discrete function, as shown in equation (9), by $G_{RC}(z)$, according to [18]:

$$G_{RC}(z) = K_{rc}\frac{z^{-N}Q(z)G_f(z)}{1-z^{-N}Q(z)}, \tag{13}$$

where N is defined as:

$$N = \frac{f_{sw}}{f_o}, \tag{14}$$

and f_o is the grid frequency. K_{rc} is the control parameter of the $G_{RC}(z)$ and m is the phase-lead number, which is determined by experiments in practice [18].

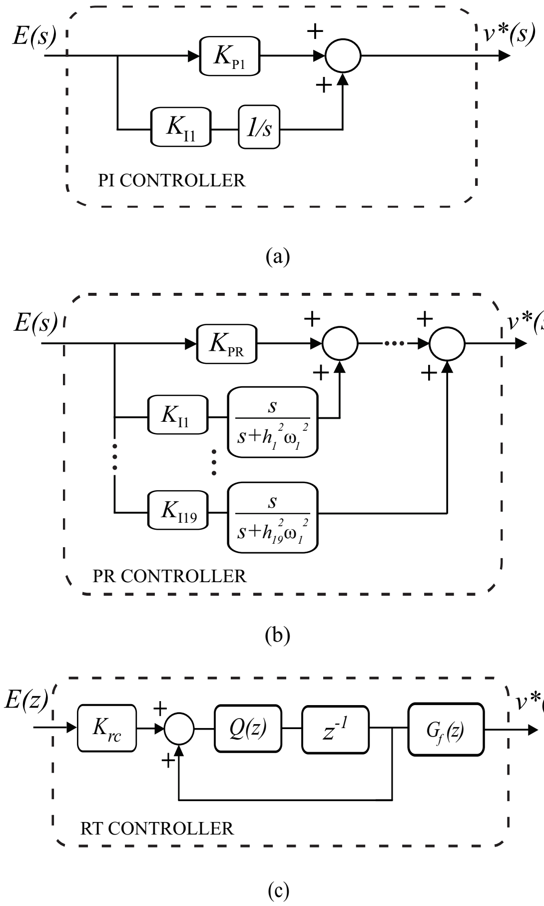

Fig. 3. Controllers used in the current loop: (a) PI (b) PR (c) RT.

All output control signals v^* are modulated and sampled, by a gain and unit order delay. The gain modulation is expressed by:

$$K_{mod} = \frac{V_{cm}}{V_{dc}}. \tag{15}$$

IV. Modulation Strategies

In most applications of integrated systems, the existence of components with different levels of operating voltages requires the need to control the output voltage. A widely used technique in converting voltage levels is the pulse width modulation (PWM), which consists of comparing two signals, one of low frequency (reference) and the other of high frequency (carrier), resulting in an alternating signal with fixed frequency and variable pulse width. In this work, the PWM sinusoidal modulation techniques were implemented.

The different PWM sinusoidal modulation techniques are presented in Fig. 4. The Unipolar, Bipolar and Hybrid modulation, are shown in Fig. 4 (a), (b) and (c), respectively. The Unipolar and Bipolar modulation has a symmetrical carrier signal. On the other hand, the Hybrid modulation uses an asymmetrical positive carrier signal.

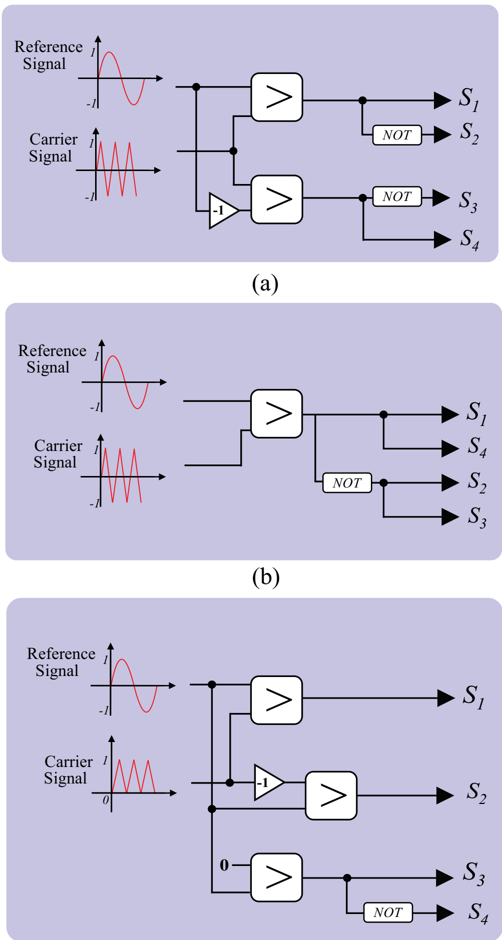

(a) (b) (c)

Fig. 4. Techniques PWM Sinusoidal Modulation: (a) Unipolar PWM (b) Bipolar PWM (c) Hybrid PWM.

In order to study the discretization methods, all controllers under study were implemented in their discretized form. In this way, the PI controllers will be studied in three cases of discretization, as shown below, and modulation techniques.

$$s = \frac{z-1}{T}, \text{ Forward.} \tag{16}$$

$$s = \frac{z-1}{zT}, \text{ Backward.} \tag{17}$$

$$s = \frac{2}{T}\frac{z-1}{z+1}, \text{ Trapezoidal.} \tag{18}$$

The other controllers are studied in terms of modulation techniques. The use of the PI controller can be justified by its easier implementation. In addition, the parameters design can be done with standard methodologies, while in PR and RT many works have proposed methodologies to tune the controllers gain [15], [16], [18], [19]. The discretization of the PR as shown in (19).

$$s = \frac{h_n w_1 (z-1)}{tg(0.5 h_n w_1 T)(z+1)}. \tag{19}$$

V. Case Study

The main circuit parameters of the DG system are presented in Tab. I.

TABLE I
System Parameters.

Parameters	**Value**
Rated Power (S_n)	3.5 kVA
Grid voltage (V_g)	230 V
Grid current (i_g)	10 A
Line frequency (f_0)	50 Hz
dc-bus voltage (V_{dc})	400 V
Line Resistance (R_g)	0.06 Ω
Line Inductance (L_g)	0.3 mH
Filter Capacitance (C_f)	5 μF
Filter Inductance (L_f)	2 mH
Filter Inductance-Resistance (R_{Lf})	0.1 Ω
Carrier frequency (f_{cm})	16 kHz
Switching frequency (f_{sw})	16 kHz
Sampling frequency (f_s)	32 kHz
Carrier Magnitude (V_{cm})	7.5 V
Ambient Temperature (T_a)	313 K

The controllers parameters are shown in Tab. II. These parameters are based on [10]. Also, they were kept the same for both modulation techniques studied in this work. The value of K_{In} is applied for n = 1, 5, 7, 11, 17 and 19.

TABLE II
Controllers Parameters.

PI Controller	**Value**
K_{P1}	12.27
K_{I1}	8533.33
K_{d1}	14
K_{mod}	0.0187
PR Controller	**Value**
K_{PR}	11.37
K_{In} (for n $\neq$ 1)	500
K_{In} (for n = 1)	1000
K_{d2}	14
K_{mod}	0.0187
RT Controller	**Value**
K_1	12.27
K_{rc}	2
N	320
m	3
α_0	0.5
α_1	0.25
K_{d3}	14
K_{mod}	0.0187

The frequency response (Bode diagram), in magnitude and phase, of the analyzed controllers and the plant (which relates i_L and v_{cf}) are presented in Fig. 5. It is possible

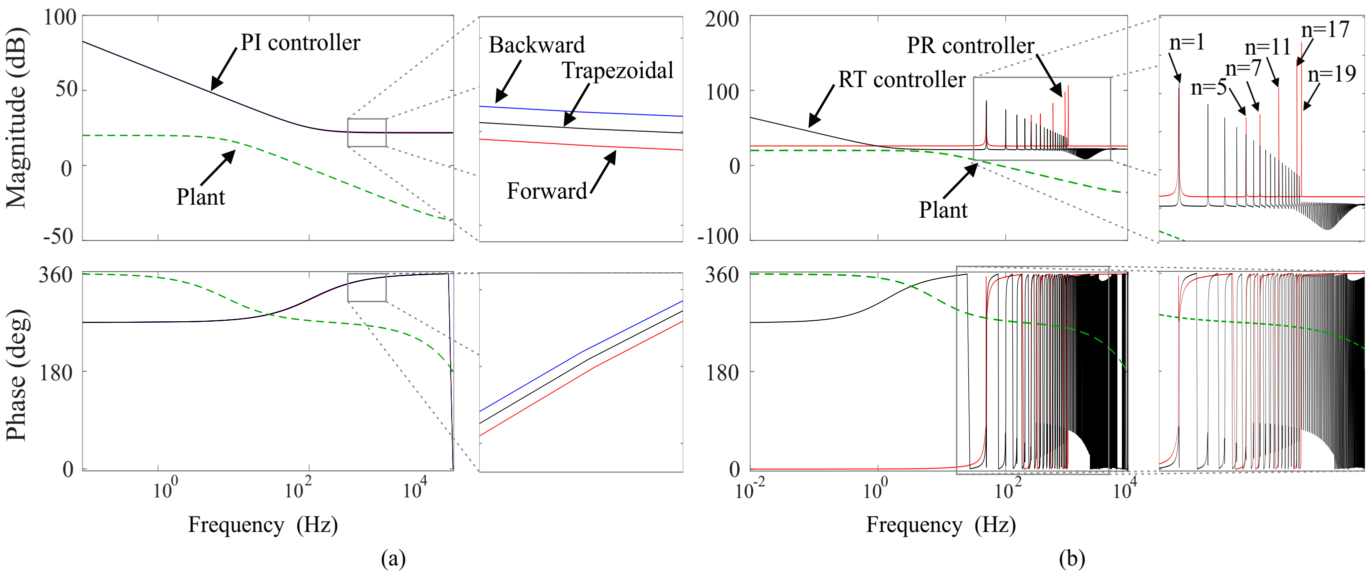

Fig. 5. Bode Diagram of the Controllers: (a) Magnitude and phase response of PI controller and plant (b) Magnitude and phase response of PR and RT controllers and plant.

TABLE III
FOSTER THERMAL IMPEDANCE FOR SEMICONDUCTORS.

Thermal impedance		$Z_{n,(j-c)}$ 1	2	3	4	5
IGBT	R (K/W)	0.0498	0.5717	0.6247	0.1199	0.0187
	τ (s)	4.7e-05	0.00048	0.0034	0.0221	0.1932
Diode	R (K/W)	0.0336	0.3365	0.6347	0.587	0.0413
	τ (s)	1.8e-05	0.00018	0.00097	0.0057	0.0784

to see the frequency response of the PI controller, in Fig. 5 (a), for the three discretization methods: Forward, Backward and Trapezoidal. In Fig. 5 (b), the PR and RT controller is presented, where the resonance frequencies are highlighted for the PR controller.

In order to compare the power losses of the semiconductors devices in the inverter, the thermal aspects of the semiconductors devices are included. The power losses consider the values of switching and conduction losses of IGBT's and diodes. Through the datasheet, it was possible to enter values of switching losses (turn on and turn off), conduction losses and the thermal impedance considering the Foster model of the power devices with part number IGB15N65S5 (IGBT) and IDP15E65D2 (diode) from Infineon. The Foster thermal impedance for semiconductors are shown in Tab. III. The heat sink-ambient resistance considered is R_{h-a} = $0.977K/W$. The semiconductor devices used are of silicon carbide technology.

Simulations were performed in PLECS environment, aiming to make the comparison among the types of discretized controllers. For the studied models, the injected grid current of 10A and $f_o = 50$ Hz are used.

In order to analyze the influence of harmonic distortion on the injected grid and verify the power quality, the TDD index was used, according to [17]. The TDD analyzes is made following the IEEE recommendation Std 519-2014. In this recommendation, the TDD accounts the ratio of the root mean square of the harmonic content, considering harmonic components up to the 50-*th* order and specifically excluding inter harmonics, expressed as a percent of the maximum demand current.

The grid voltage profile is presented in Fig. 6. At t = 0.5 seconds the grid becomes distorted, containing the following harmonic components: 20% *5-th*, 10% for *7-th*, *11-th*, *17-th* and *19-th*.

The case studies developed in this work to compare control and modulation strategies are:

- *TDD analyzes:* In this case, a study of TDD in the grid current was realized comparing three PWM sinusoidal modulation techniques and three discretization methods (Forward, Backward and Trapezoidal), considering the PI controller. For the PR and RT controllers, three PWM sinusoidal modulation techniques is studied;
- *Power Losses:* Considering the controllers, an analyzes of the inverter power losses (switching and conduction losses). A study was realized about three PWM sinusoidal modulation techniques considering this controllers and the three discretization methods presented for PI controller. For all cases, the study is made with and without the presence of harmonics in the grid. The power losses analyzes are made in radar plots, in order to compare all the modulation and discretization techniques at the same time. Modulation techniques are limited externally by the indicated arcs;
- *Grid Current Error:* The error analyzes is made in the grid current, considering the better situation in modulation techniques and the discretization methods for each one controller;
- *Influence of the Grid Short-Circuit:* In this case, the influence of the grid short-circuit level on the TDD is

analyzed. For this, the grid impedance was gradually reduced and increased with a short circuit factor (γ).

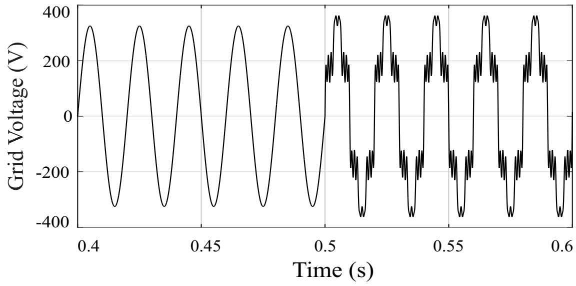

Fig. 6. Grid Voltage with and without harmonics distortion.

In order to analyze the performance of the controller under different short circuit conditions, the grid impedance (Z_g) is varied with a short circuit factor (γ):

$$Z_g = R_g\gamma + j2\pi f_0 L_g\gamma, \tag{20}$$

The analyzes considers the maximum and minimum values that guarantee the stability of the grid current control, analyzing aspects of TDD and waveforms.

VI. Results

Fig. 7 presents the results of the harmonic distortion rate of the mains current using the PI, PR and RT controllers, for the three modulation techniques (all controllers) and three discretization methods (PI controller). It is possible to verify in Fig. 7 (a) e (b), respectively, that the Unipolar and Bipolar modulation presents similar results, for all controllers.

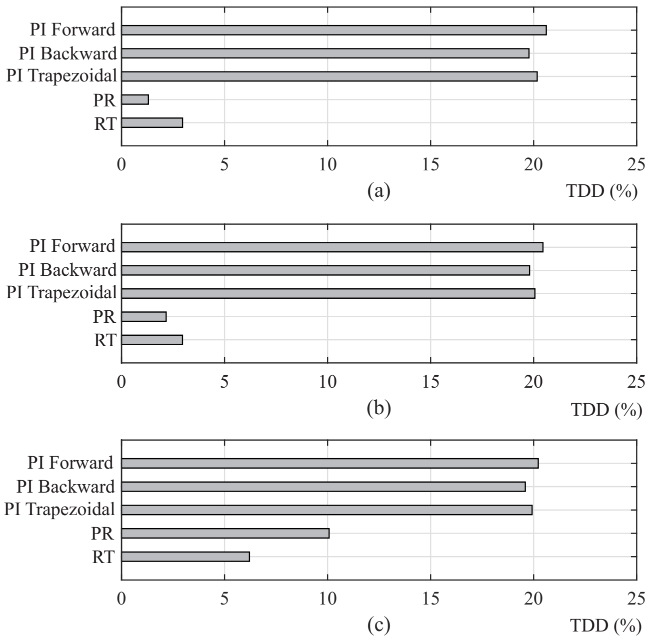

Fig. 7. TDD Analyzes - PI, PR and RT controllers; (a) Unipolar (b) Bipolar (c) Hybrid Modulations (grid distortion: 20% *5-th*, 10% for *7-th*, *11-th*, *17-th* and *19-th*).

The Hybrid modulation is presented in Fig. 7 (c). The Hybrid modulation showed, in relation the others modulation techniques, similar distortion in TDD level for PI and considerable increased for PR and RT controllers.

It is therefore understood that the PR and RT controllers have shown better performance in terms of distortion by harmonic components, which may be justified by its very nature of attenuating specific harmonic components. The PI controller, presented the worst performance, with approximately five times greater in relation of the distortion controllers RT and PR for Unipolar and Bipolar modulations. Furthermore, presents two times greater in relation to the PR controller and three times greater for the controller RT for a Hybrid modulation. Only the PR and RT controllers, for unipolar and bipolar modulations, remained on the recommendation of 5% of TDD, proposed in [17].

Fig. 8 shows the power losses (conduction and switching losses) of the semiconductors devices, with the presence grid harmonic distortion. It can be noticed that the values of losses are very close, when compared with the power inverter, being close to 0.01 pu, for all controllers. Moreover, for all controllers Hybrid modulation presents smaller power losses.

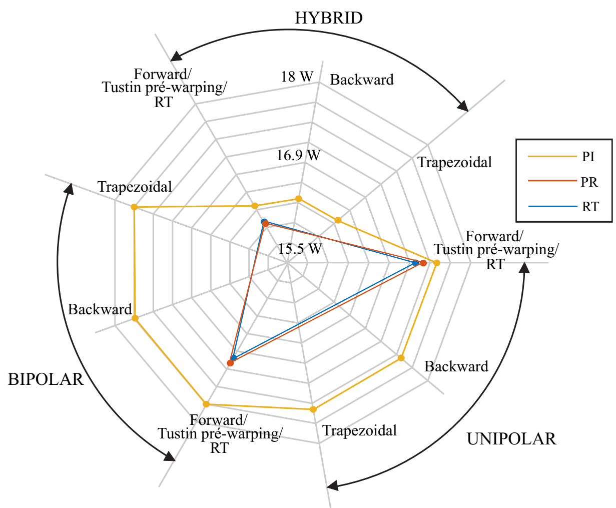

Fig. 8. Power Losses (with Grid Harmonic Distortion).

It is possible to see that the power losses, for the PI controller, are almost the same considering all discretization methods. In this case, the Trapezoidal discretization and a Hybrid modulation presents smaller power losses. The RT and PR controllers presents the lower losses, compared with the PI controller.

In order to verify the influence of grid distortion, the power losses were calculated for the same cases, of modulation and discretization, among the three controllers analyzed. Fig. 9 shows this analyzes. It is possible to see that the power losses follow the same proportions as the previous case analyzed, with minimal differences between the values of power losses for each case. In this way, it is verified that the presence of harmonic distortion had small impact influence on the losses.

Evaluating the results of power losses and TDD, it is verified that if the best cases of modulation strategies and discretization methods, for each controller:

- PI Controller: Hybrid Modulation and Backward Discretization;
- PR Controller: Unipolar Modulation;
- RT Controller: Unipolar Modulation;

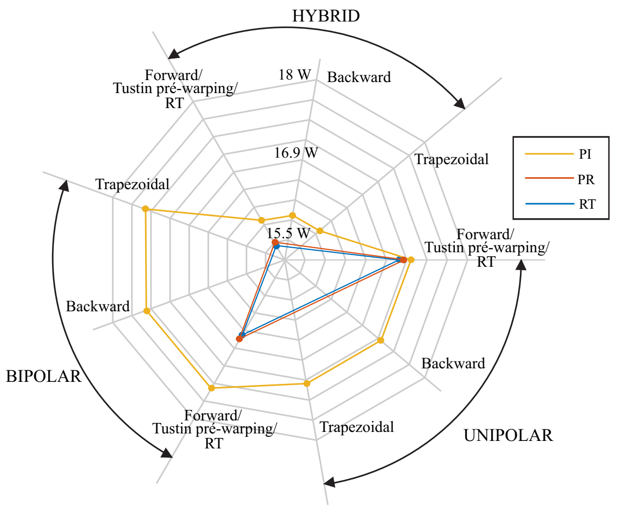

Fig. 9. Power Losses (without Grid Harmonic Distortion)

The grid current performance for the best cases of controllers are studied, to evaluate the power losses and TDD. Thus, the Fig. 10 shows the response with and without harmonics distortion. It can be verified that the waveforms of the PR and RT controllers present smaller distortions, compared with the PI controller. Highlighted, we have the RT controller that presented the lowest THD value.

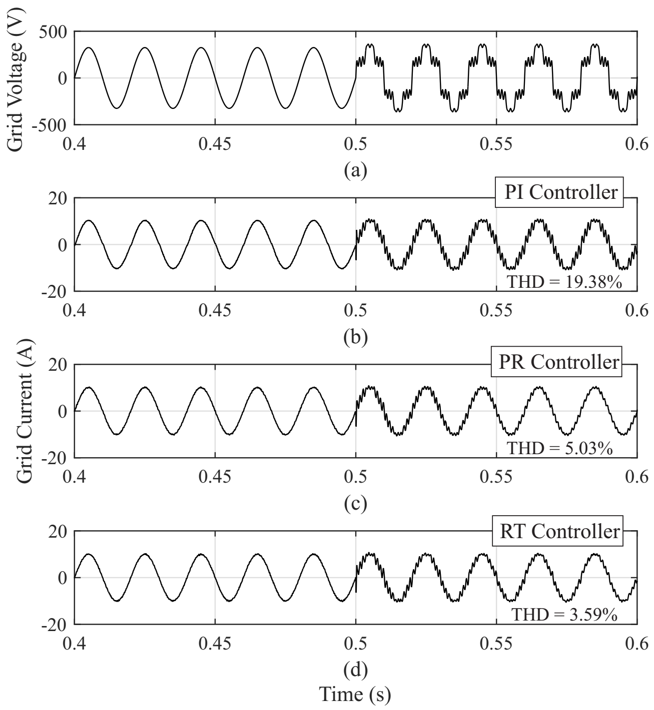

Fig. 10. Grid Voltage and Current - Types of Controller

In the Fig. 11 the current error can express the control performance of the implemented controllers. PR controller, shown in Fig. 11 (b) presents the best performance in relation the others, with a small signal error. The RT controller, Fig. 11 (c), presents similar results. The PI controller presents significant peak currents both in the grid with and without harmonic.

Finally, the short circuit analyzes is done. Fig. 12 shows

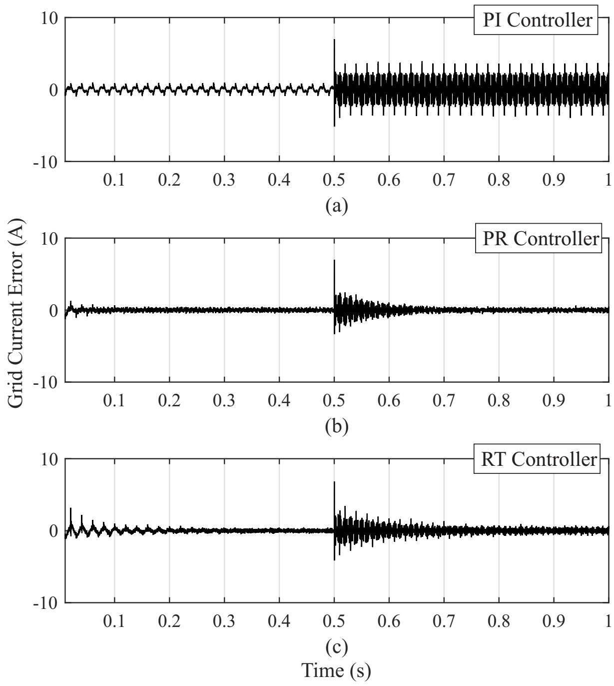

Fig. 11. Grid Current Error - Types of Controller

the grid current response for two cases of short circuit level. In this way, the factor γ represents the critical cases that the control can keep the grid current stable.

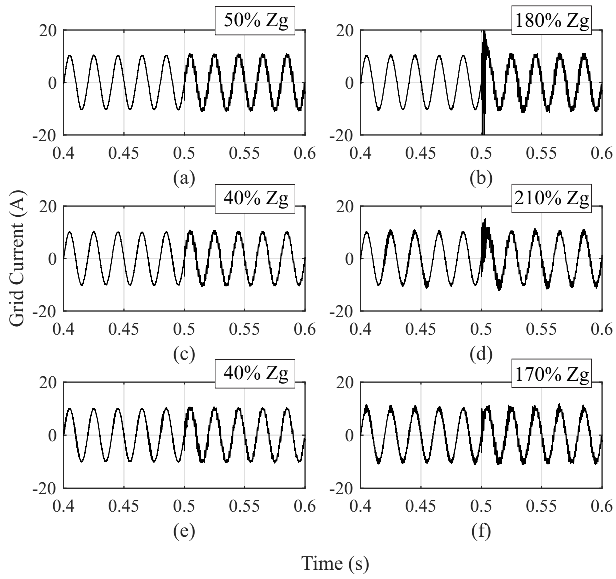

Fig. 12. Grid Current - Short Circuit Level (a), (b) PI (c), (d) PR (e), (f) RT

Another analyzes performed as a way to complete the comparison between controllers was through TDD analyzes, as shown in Tab. IV. It is possible to notice that the distortion increased with the increment in the grid impedance. In addition, it is possible to reduce the grid impedance 10 % more in the PR and RT controllers than in the PI controller. The PI was the controller that allowed a greater increase in the grid impedance.

TABLE IV
VARIATION OF THE TDD (%) WITH THE CONSTANT γ.

	Percentage of Zg and TDD							
Controller Type	γ (%)	TDD	γ (%)	TDD	γ (%)	TDD	γ (%)	TDD
PI	50	19.6785	75	19.7365	140	19.7718	180	21.4603
PR	40	1.2090	75	1.4195	140	1.6570	210	3.2759
RT	40	2.9059	75	2.91	140	3.0049	170	6.1502

VII. CONCLUSION

This work presented an analysis on the impacts of different forms of modulation strategies and discretization methods in a DG inverter. The analyzes involved the comparison among PI, PR and RT controllers. The dc-link voltage, power semiconductor stresses and grid filter were designed for a 3.5-kVA DG inverter.

In terms of power losses, the results showed an equality between the discretization methods, when compared each modulation techniques separately. The PR and RT controllers presents the lower power losses in Hybrid modulation. On the other hand, the TDD rate revealed the Hybrid modulation is a poor in grid current quality, outside the IEEE recommendation. The short circuit analyzes presented a lower TDD varying the short circuit factor, in PR and RT controller. Finally, the study of different types of controllers revealed an excellent response of the PR and RT controllers in the grid energy quality, for unipolar modulation and hybrid modulation for PI controller.

Additionally, modulation methods and controllers implemented showed high impact on the grid quality, with emphasis on the hybrid modulation technique in PR and RT controller. The joint use has revealed potentials for framing standards international of harmonic limits in the grid current. The analyzes carried out validated ways to increase the performance, mainly thinking in large applications where the power of the system is higher and generates greater losses and harmonics impact. As a proposal for the continuity of this work, it is indicated the joint implementation of the PR controller with RT, as presented in [13], [18] (in order to increase the quality of the grid system), a study of the influence of the frequency of sampling on the performance of the system and a study of the cost of implementation in DSP's, for practical validation.

REFERENCES

[1] E. Nazerian, S. Gharebaghi, and A. Safdarian, "Optimal distribution network reconfiguration considering power quality issues, in 2017 Smart Grid Conference (SGC), Dec 2017, pp. 16.

[2] R. O. Anurangi, A. S. Rodrigo, and U. Jayatunga, "Effects of high levels of harmonic penetration in distribution networks with photovoltaic inverters, in 2017 IEEE International Conference on Industrial and Information Systems (ICIIS), Dec 2017, pp. 16.

[3] J. G. Slootweg and W. L. Kling, "Impacts of distributed generation on power system transient stability," IEEE Power Engineering Society Summer Meeting,, Chicago, IL, USA, 2002, pp. 862-867 vol.2.

[4] P. Chiradeja, "Benefit of Distributed Generation: A Line Loss Reduction Analysis," 2005 IEEE/PES Transmission & Distribution Conference & Exposition: Asia and Pacific, Dalian, 2005, pp. 1-5.

[5] J. K. Phipps, J. P. Nelson, and P. K. Sen, "Power quality and harmonic distortion on distribution systems, IEEE Transactions on Industry Applications, vol. 30, no. 2, pp. 476484, Mar 1994.

[6] Q. Qian, J. Xu, S. Xie and L. Ji, "Analysis and improvement of Harmonic Quasi Resonant control for LCL-filtered grid-connected inverters in weak grid," 2016 IEEE Applied Power Electronics Conference and Exposition (APEC), Long Beach, CA, 2016, pp. 3446-3452.

[7] F. Wang, X. Feng, L. Zhang, Y. Du and J. Su, "Impedance-based analysis of grid harmonic interactions between aggregated flyback micro-inverters and the grid," in IET Power Electronics, vol. 11, no. 3, pp. 453-459, 3 20 2018.

[8] C. R. Baier, M. A. Torres, P. Acuna, J. A. Muoz, P. E. Meln,C. Restrepo, and J. I. Guzman,, "Analysis and design of a control strategy for tracking sinusoidal references in single-phase grid-connected current-source inverters," IEEE Transactions on Power Electronics, vol. 33, no. 1, pp. 819832, Jan 2018.

[9] D. R. Joca, L. H. S. C. Barreto, D. de S. Oliveira, P. P. Praca, R. N. A. L. Silva, and G. A. L. Henn, "THD analysis of a modulation technique applied for thd reduction," in 2013 Brazilian Power Electronics Conference, Oct 2013, pp. 177182.

[10] F. Wang, J. L. Duarte, M. A. M. Hendrix, and P. F. Ribeiro, "Modeling and analysis of grid harmonic distortion impact of aggregated dg inverters, IEEE Transactions on Power Electronics, vol. 26, no. 3, pp. 786797, March 2011.

[11] Z. Rymarski and K. Bernacki, "Different approaches to modelling single-phase voltage source inverters for uninterruptible power supply systems, IET Power Electronics, vol. 9, no. 7, pp. 15131520, 2016.

[12] T. Guofei, X. Guochun, Z. Zhibo, and L. Yong, "A control method with grid disturbances suppression for a single-phase lcl-filter-based grid-connected inverter, in 2012 Twenty-Seventh Annual IEEE Applied Power Electronics Conference and Exposition (APEC), Feb 2012, pp.14891493.

[13] Y. Yang, K. Zhou, and F. Blaabjerg, "Current harmonics from single phase grid connected inverters; examination and suppression, IEEE Journal of Emerging and Selected Topics in Power Electronics, vol. 4, no. 1, pp. 221233, March 2016.

[14] P. Yu, M. Wu, J. She, K. Z. Liu, and Y. Nakanishi, "An improved equivalent-input-disturbance approach for repetitive control system with state delay and disturbance, IEEE Transactions on Industrial Electronics, vol. 65, no. 1, pp. 521531, Jan 2018.

[15] Y. Ye, G. Xu, Y. Wu, and Q. Zhao, "Optimized switching repetitive control of cvcf pwm inverters, IEEE Transactions on Power Electronics, vol. 33, no. 7, pp. 62386247, July 2018.

[16] S. Mukherjee, P. Shamsi, and M. Ferdowsi, "Control of a single-phase standalone inverter without an output voltage sensor, IEEE Transactions on Power Electronics, vol. 32, no. 7, pp. 56015612, July 2017.

[17] IEEE Recommended Practice and Requirements for Harmonic Control in Electric Power Systems, in IEEE Std 519-2014 (Revision of IEEE Std 519-1992), pp.1-29, June 11 2014.

[18] Y. Yang, K. Zhou, H. Wang and F. Blaabjerg, "Analysis and Mitigation of Dead Time Harmonics in the Single-Phase Full-Bridge PWM Converters with Repetitive Controllers," in IEEE Transactions on Industry Applications.

[19] A. G. Yepes, F. D. Freijedo, . Lopez and J. Doval-Gandoy, "Analysis and Design of Resonant Current Controllers for Voltage-Source Converters by Means of Nyquist Diagrams and Sensitivity Function," in IEEE Transactions on Industrial Electronics, vol. 58, no. 11, pp. 5231-5250, Nov. 2011.

[20] R. Pea-Alzola, M. Liserre, F. Blaabjerg, M. Ordonez and Y. Yang, "LCL-Filter Design for Robust Active Damping in Grid-Connected Converters," in IEEE Transactions on Industrial Informatics, vol. 10, no. 4, pp. 2192-2203, Nov. 2014.

[21] S. G. Parker, B. P. McGrath and D. G. Holmes, "Regions of Active Damping Control for LCL Filters," in IEEE Transactions on Industry Applications, vol. 50, no. 1, pp. 424-432, Jan.-Feb. 2014.